



This is to certify that the

thesis entitled

TOPOGRAPHIC EFFECTS ON THE NORMALIZED DIFFERENCE VEGETATION INDEX, ROCKY MOUNTAIN NATIONAL PARK, COLORADO presented by

David Frota Vaughan

has been accepted towards fulfillment of the requirements for

M.A. degree in Geography

Major professor

Date 8/7/96

MSU is an Affirmative Action/Equal Opportunity Institution

O-7639

LIBRARY Michigan State University

PLACE IN RETURN BOX to remove this checkout from your record. TO AVOID FINES return on or before date due.

DATE DUE	DATE DUE	DATE DUE

MSU is An Affirmative Action/Equal Opportunity Institution choirdatedus.pm3-p.1

TOPOGRAPHIC EFFECTS ON THE NORMALIZED DIFFERENCE VEGETATION INDEX, ROCKY MOUNTAIN NATIONAL PARK, COLORADO

Ву

David Frota Vaughan

A THESIS

Submitted to
Michigan State University
in partial fulfillment of the requirements
for the degree of

MASTER OF ARTS

Department of Geography

1996

ABSTRACT

TOPOGRAPHIC EFFECTS ON THE NORMALIZED DIFFERENCE VEGETATION INDEX, ROCKY MOUNTAIN NATIONAL PARK, COLORADO

Ву

David Frota Vaughan

The normalized difference vegetation index (NDVI) has become widely accepted because of its compensation for changing illumination conditions and simplicity (Lillesand and Kiefer, 1994). Although NDVI compensates, partially, for the effects of topography on remote sensing measurements, the question remains whether signal noise, attributed to the remaining topographic effect, may explain variability in NDVI. Greater understanding of the remaining topographic effect may yield more accurate interpretation of NDVI in sensitive ecotones. Through the examination of NDVI, solar incidence angle, and known vegetation cover for a site in Rocky Mountain National Park, this thesis explores the question of whether the calculated NDVI values are related to topography and how strong is that relationship, if any, relative to the vegetation influence. Statistical tests indicate a significant relationship between incidence angle and NDVI. In large, homogeneous areas, the "noise" of incidence angle may account for up to 6% of the NDVI signal.

To my mother,
for encouraging me to continue
my education

ACKNOWLEDGMENTS

I wish to thank my advisor, Dr. Daniel Brown, for his continued support, encouragement, and guidance throughout this research effort. In addition, I am grateful for the support of Dr. Jay Harman and Dr. David Lusch, who gave willingly of their time and expertise in order for me to complete the project.

Several others deserve to be mentioned. I would like to thank

Dr. Bruce Pigozzi for his patient and helpful explanations. Mike

Lipsey gave generously of his time whenever called upon.

Finally, I want to acknowledge Nat, Cath, Claudia, Dee, Jim, and Reina for there ever-present friendship and unwavering support throughout this project.

TABLE OF CONTENTS

LIST OF TA	BLES vii
LIST OF FIG	GURES viii
CHAPTER:	
1. INTROD	UCTION AND RESEARCH QUESTION1
1.1	Remote sensing of vegetation1
1.2	Linking vegetation characteristics and radiance4
1.3	Vegetation indices5
1.4	Background: Terrain's effect on remote sensing7
1.5	Problem11
1.6	Research question
2. SITE DES	SCRIPTION 1 5
2.1	Study area1 5
3. DATA Al	ND METHODS1 9
3.1	Addressing the research question
3.2	Data
	3.2.1 Landsat Thematic Mapper image20
	3.2.2 Digital elevation model (DEM)22
	3.2.3 Vegetation cover map22
3.3	Preparing the data24
	3.3.1 Generating NDVI24
	3.3.2 Calculating incidence angle28
	3.3.3 Shadow map

	3.3.4 Vegetation reclassification	3 3
	3.3.5 Raw and classed cos(i)	4 1
3.4	Methods	4 2
	3.4.1 Sampling the data	4 2
	3.4.2 Statistical techniques	
IV. RESUL	TS	4 8
4.1	Statistical results	4 8
V. DISCUS	SSION AND CONCLUSIONS	5 3
5.1	Discussion	5 3
5.2	Concluding remarks	5 6
	Future research	
VI. APPEN	DICES	5 9
A.	Characteristics of the Landsat TM	5 9
В.	Meta data of the Landsat image	60
VII ITED	ATTIRE CITED	6.1

LIST OF TABLES

е	
Correction of the topographic effect	
by cosine manipulation	1 0
Basic and modified vegetation indices	1 2
Original groundcover classifications for Rocky Mountain	
National Park	2 3
Vegetation cover classes	34
Forest density classifications	3 5
Reclassified cover classes from original vegetation map	37
Final classifications of composition/density classes	3 8
Classification of cos (i), range 0 - 1	4 1
Vegetation class occurrence within incidence classes	47
ANOVA results for vegetation	
and incidence angle groups	4 9
Regression results for	
final 33 vegetation/density classes	5 1
	Correction of the topographic effect by cosine manipulation

LIST OF FIGURES

Figure Deciduous and coniferous tree spectral signatures, 1.1 range 0.4 μm - 0.9 μm3 2.1 Study area in Rocky Mountain National Park......16 Landsat TM image bands 4, 3, and 2 3.1 displayed in RGB......21 NDVI image generated from radiance values......27 3.2 3.3 3.4 Vegetation/density classification map and legend.....39, 40 3.5

CHAPTER 1

INTRODUCTION AND RESEARCH QUESTION

1.1 Remote sensing of vegetation

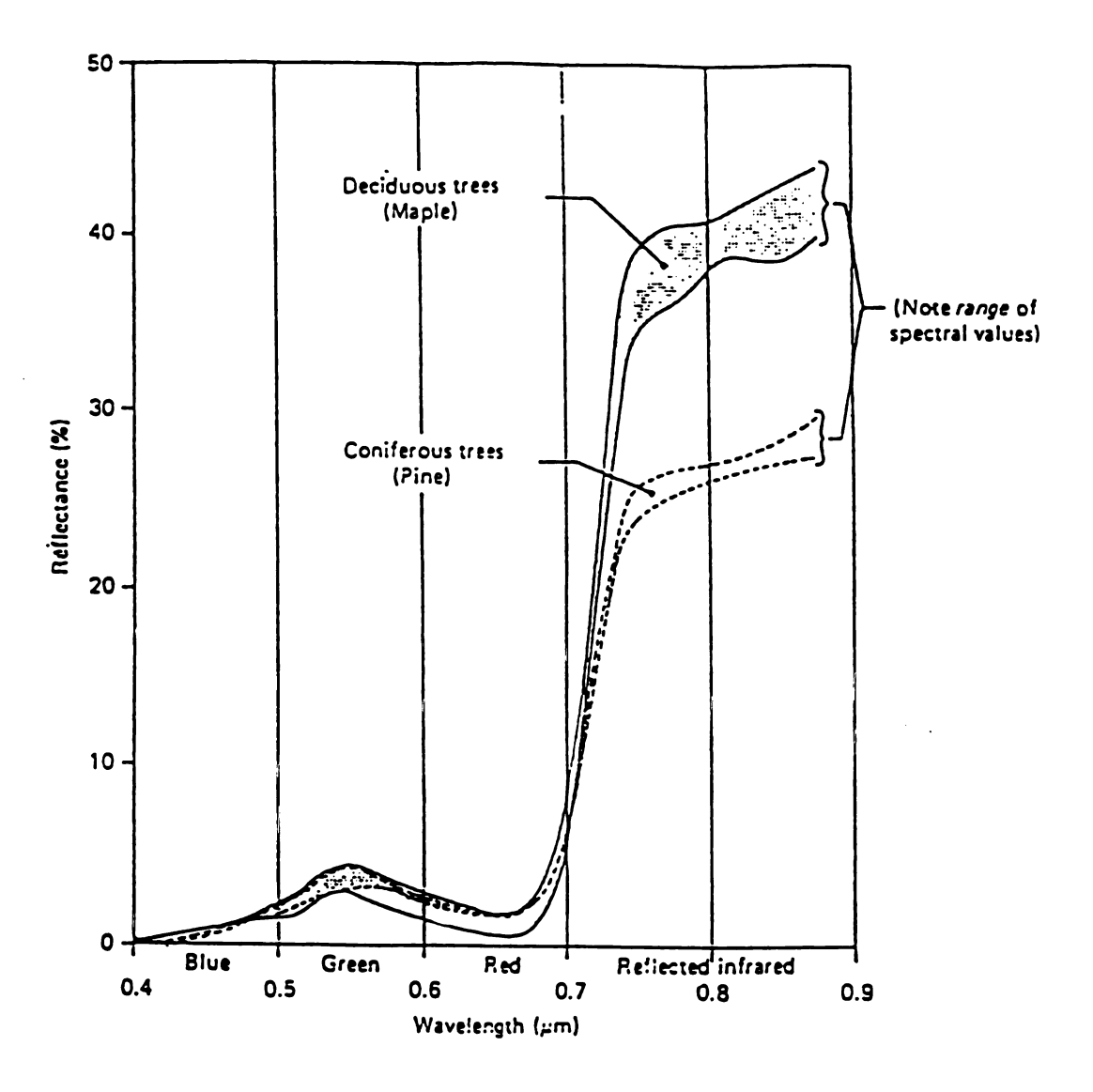
Vegetation can be studied without physical contact or direct observation because of its interaction with electromagnetic radiation. Remote sensing is the science and art of obtaining information about an object, area, or phenomenon through the analysis of data acquired by a device that is not in contact with the object, area, or phenomenon under study (Lillesand and Kiefer, 1994). This concept is now extended to include sensors aboard earth-orbiting satellites.

Electromagnetic energy registered by a passive remote sensor¹ originates primarily from the sun. As incoming solar electromagnetic radiation (EMR) interacts with the earth's atmosphere, three paths are possible: absorption by water or aerosols in the atmosphere, reflection by clouds back into space, or transmission through the atmosphere to the ground. Of the energy that encounters the ground, some is absorbed and some energy is reflected by ground cover. The reflected energy will be directed back through the atmosphere and, possibly, to an earth-orbiting remote sensing satellite. What is received by the satellite is known as radiance, the total of energy radiated by a unit area per solid angle of measurement (Lillesand and Kiefer, 1994). Not all ground

A passive sensor does not provide its own electromagnetic energy source.

cover (e.g., vegetation) will interact with incoming EMR in the same manner. The proportion of radiation that is reflected will vary with both vegetation type and the portion of EMR (i.e., band wavelength) in which the vegetation is being observed. The unique relationships between vegetation characteristics and reflectance in the visible and near-infrared portions (i.e., wavelengths of $0.4 - 0.9 \mu m$) of the EM spectrum enable a passive satellite to efficiently record information about vegetation.

The depiction of an object's reflectance characteristics across a range of EMR is known as its "spectral signature." The reflectance for vegetation peaks in two separate wavelength ranges: the green $(0.5 - 0.6 \mu m)$ and near-infrared $(0.7 - 0.9 \mu m)$ portions of the spectrum (Figure 1.1). Reflectance within the green portion of the spectrum is due to plant pigmentation (Lillesand and Kiefer, 1994). Overall reflectance of visible light energy is diminished due to the presence of chlorophyll-a and -b, which are highly absorptive of red and blue light. In comparison with visible wavelengths, relative reflectance from vegetation in near-infrared wavelengths is much greater. Reflectance from plants within the near-infrared portion of the spectrum is controlled by internal leaf structure. Large airpockets within the leaf enable reflection of the longer wavelengths (Curran, 1985; Gausman, 1977; Lillesand and Kiefer, 1994). Given sufficient spatial detail of the sensor, variation in internal leaf structure and leaf morphology creates variations in spectral signatures large enough to enable the classification of vegetation, especially between major classes such as deciduous and coniferous trees, from spectral information alone.



(Adapted from Kalensky and Wilson, 1975).

Figure 1.1. Deciduous and coniferous tree spectral signatures, range 0.4 μm - 0.9 μm .

Other physical characteristics of vegetation affect the amounts of EM energy reflected, absorbed, and transmitted by an individual plant. Water content within the leaf, plant maturity and senescence, and the presence of disease will all alter the pigmentation and/or the structure of leaves and, thus, the amount of energy reflected (Curran, 1985).

1.2 Linking vegetation characteristics and radiance

Reflected radiance measurements are related to physical properties of vegetation over extents larger than individual plants (e.g., of communities) if the ground resolution cell of the imaging radiometer is much greater than the individual plant. Vegetation type characteristics such as biomass, leaf area, species, and stress have known effects on spectral response (Perry and Lautenschlager, 1984). Biomass is defined as the total amount of vegetation within a specified region (Perry and Lautenschlager, 1984). Leaf Area Index (LAI) is defined as the cumulative leaf area per unit on the ground (Price, 1993).

The first to make the link between physical characteristics of vegetation and radiance was Jordan (1969), who incorporated vegetation response characteristics in the near-infrared (~0.8 μm) and red (~0.675 μm) regions of EMR to derive, using a ratio of the two bands, a measure of LAI (c.f., Tucker, 1979). Further development of ratios between infrared and red radiance, as reported by Tucker (1979), included the works of Colwell (1973) and Rouse et al. (1973, 1974). Colwell (1973) determined that the ratio of infrared to red radiation normalized variation in soil

background reflectance and "was useful for estimating biomass" (Tucker, 1979, p.128.).

1.3 <u>Vegetation indices</u>

It was Rouse et al. (1974) who defined the term "vegetation index": the ratio of radiance in one spectral band to that of another for a particular satellite sensor (cf., Tucker, 1979). In general, a vegetation index is a composite measure of spectral radiance recorded in both the red and near-infrared regions of the electromagnetic spectrum. Indices take advantage of the differences in the spectral response characteristics of vegetation in each of these wavelength channels. An index, therefore, summarizes information recorded within several wavelength channels into one variable/image that is representative of broad vegetation characteristics such as species, leaf area, stress, or biomass (Curran and Wardley, 1988; Perry and Lautenschlager, 1984). A wavelength channel of a particular satellite sensor is that portion of the EM spectrum to which a sensor channel is sensitive. In the case of Rouse et al. (1974), the sensor was the Multispectral Scanner (MSS) of the early Landsat program and the index was calculated by combining MSS channels 2 and 4 $(0.6 - 0.7 \mu m \text{ and } 0.8 - 1.1 \mu m, \text{ respectively}).$

Early tests were performed to evaluate the relationships between vegetation indices and vegetation (Tucker, 1979). Many indices were "sensitive to the amount of photosynthetically active vegetation present in the plant canopy" (Tucker, 1979, p. 134). The width of the red and near-infrared band was shown to have little

effect on the radiance received, and thus, the derived vegetation information. One effective index tested by Tucker (1979) was the difference ratio:

(Infrared - Red) / (Infrared + Red)

This difference ratio became known as the normalized difference vegetation index (NDVI) and has been widely utilized. Throughout the development and testing of vegetation indices, combinations of red and infrared were shown to be superior to the earlier ratios of red and green in extracting canopy variables (Tucker, 1979).

Applications of vegetation indices have included monitoring areally extents of food crops (Baret and Guyot, 1991; Guttman, 1991). The importance of global food production has led to the daily monitoring of vegetation by the National Oceanic and Atmospheric Association (NOAA) satellites, carrying the Advanced Very High Resolution Radiometer (AVHRR). This instrument gathers data in the red and infrared portions of the spectrum (Lillesand and Kiefer, 1994), in addition to longer wavelength channels. The ground resolution element (GRE) of an orbiting satellite system is the area of land that the scanning sensor "sees" at any given time and is equivalent to its spatial resolution. The GRE for the NOAA series of satellites is 1.2 km². At such a resolution, the reflected radiance, and therefore vegetation cover information, is summarized with one value for an entire square kilometer. AVHRR is appropriate for depicting large farming systems, such as those present in the United States, because of the large areal extents of the crop cover patches. The reduction of the data that occurs when vegetation indices are used to summarize radiance recorded in

multiple wavelength channels allows for daily regional assessment of crop phenology throughout the growing season (Brown et al., 1993). The data reduction also enables global vegetation monitoring (Goward et al., 1993; Gutman, 1991). The significance of applications of vegetation indices to cropland is matched by applications to forests and natural areas. In many naturally vegetated areas, the ground is not as flat as cropland. More undulating topography may have an impact upon the applications of vegetation indices, specifically NDVI.

1.4 Background: Terrain's effect on remote sensing

The topography of a region serves to inhibit the simple application of spectral information derived from orbiting multispectral scanner data (Karaska et al., 1986.) Many applications to agriculture are not affected by topography due to the generally flat nature of farmland. However, for non-agricultural applications, specifically forestry, the influences of topography can complicate interpretations (Leprieur et al., 1988, Meyer et al., 1993).

Variability in topography appears as differences in elevation, hill slope, and aspect, the orientation of a slope face. Terrain variability influences the amount of solar radiation striking any given location by inducing shadowing and shading (Dubayah and Rich, 1995). The geometric relationship between the Sun's position in the sky and the orientation of the landscape will vary from one location to another. Under clear sky conditions solar illumination angle can be used to explain the amount of solar irradiance for any given location on a landscape (Dubayah and Rich, 1995). Terrain

surrounding a given location may block direct solar radiation from reaching that place: the area is, therefore, in shadow. Shading, on the other hand, is a measure of the strength of the direct solar radiation received at any given landscape position at some specified date and time.

The impact of topography on multispectral sensor measurements is termed the topographic effect: a phenomenon that alters spectral reflectance from similar cover types due to variations in slope and aspect of the terrain (Holben and Justice, 1980). The result is a greater variance than expected in satellite-generated digital numbers (DN) for any given vegetation type due to variations in terrain conditions. Digital numbers are the nominally-scaled measurements at each of the satellite's sensors and must be corrected for slight imbalances between each of the detectors in order to calculate radiance (EOSAT NOTES, 1994).

A correction factor, based on the solar incidence angle and the differences in radiance from a given cover type between flat and inclined surfaces, may be calculated and applied to the original scene to ameliorate the topographic effect. Solar incidence angle for any given location within a landscape may be determined with the use of a digital elevation model, a geometric representation of the terrain surface using a grid system. The terrain orientation may then be compared to sun positions to determine solar incidence angle for each cell within the grid. The topographic correction reduces the variance of measured radiance within known cover types due to variations in topography. As a result, greater accuracy

is achieved by computer-conducted landcover classifications of digital numbers (Civco, 1989; Teillet et al., 1982).

Attempts to correct for the topographic effect have taken different forms. First, topographic data, and calculated maps of incidence angle, have been used to adjust the digital numbers directly (Civco, 1989; Frank, 1988; Holben and Justice, 1980; Meyer et al., 1993) (Table 1.1). Although it is theoretically possible to do a topographic correction to individual bands prior to NDVI calculation, applications of NDVI do not include such manipulations, historically. Topographically corrected data have not been used to calculate NDVI because the topographic effect is wavelength dependent and ratios of multiple topographically corrected bands may introduce unknown biases into the derived values. In addition, the topographic effect is reduced significantly by the nature of the formulation of the NDVI.

The concept of using a ratio to reduce the topographic effect was effectively demonstrated by Holben and Justice (1981). In tests comparing red and infrared radiance values, ratios of individual bands effectively reduced the topographic effect by a factor of six (Holben and Justice, 1981). It was also reported that if directional reflectance properties were wavelength dependent, spectral band ratioing did not completely reduce the topographic effect (Hoblen and Justice, 1981). In order for a ratio to be correct in its application to reduce topographic influence, whether using single bands or difference ratios, converting DNs to radiometric units facilitates the accurate computation of NDVI (Price, 1987).

Table 1.1. Correction of the topographic effect by cosine manipulation.

Correction Method	Remarks
Statistic-empirical correction $L_{H} = L_{T} - \cos(i) \cdot m$	Purely statistical approach based on a linear relationship between the original band and the illumination. Geometrically the correction rotates the regression line to the horizontal to remove the illumination dependence.
Cosine correction $L_{H} = L_{T} \left[\frac{\cos(sz)}{\cos(i)} \right]$	Trigonometric approach taking into account the portion of direct irradiance on the inclined surface element (pixel). Objects are regarded as Lambertian reflectors.
Minnaert correction (semi-empirical) $L_{H} = L_{T} \left[\frac{\cos(sz)}{\cos(i)} \right]^{k}$	Variation of the cosine correction by introduction of a Minnaert constant, simulating the non-Lambertian behaviour of the earth surface. With k=1 it is a normal cosine correction.
C-correction (semi-empirical) $L_{H} = L_{T} \left[\frac{\cos(sz) + c}{\cos(i) + c} \right]$	Modification of the cosine correction by a factor c which should model the diffuse sky radiation. c is based on the regression in the statistic-empirical approach.

where:

LH = radiance observed at horizontal surface
LT = radiance observed over sloped terrain
sz = solar zenith angle
i = sun's incidence angle
k = Minnaert constant
c= b/m = correction parameter
m= inclination of regression line
b= intercept of regression line

(Reprinted from Meyer et al., 1993)

1.5 Problem

Of the many vegetation indices that have been developed, several to measure vegetation (Table 1.2), NDVI has become widely accepted because of its simplicity (Lillesand and Kiefer, 1994). Although popular and widely applied, NDVI does not compensate for all topographic effects (Guttman, 1991). Slight variations exist in the bi-directional distributions (i.e., by illumination and viewing angle) of red and near-infrared reflectance for a given landscape (Guttman, 1991).

Evaluation of NDVI, as expressed in much of the literature, is primarily focused on NDVI generated from data acquired by the AVHRR instrument on the NOAA series of polar-orbiting satellites. AVHRR imagery covers a swath width of 2400 km (Lillesand and Kiefer, 1994), making the view angle an important concern (Goward et al., 1991; Guttman, 1993). View angle is the determinant of a satellite's ability to detect surface illumination (Wardley, 1984). As the earth's surface curves away from the satellite nadir position, for any particular scan line, its ability to accurately detect surface illumination is affected (Goward, 1991).

Table 1.2. Basic and modified vegetation indices.

```
1.
      Normalized difference vegetation index (NDVI)
             = (infrared - red) / (infrared + red)
2.
      Soil adjusted vegetation index (SAVI)
             = [(infrared-red)/(infrared+red+L)] * (1+L)
             where L = soil calibration factor
3.
      Modified soil adjusted vegetation index (MSAVI)
             = { 2infrared + 1 - [(2infrared + 1)^2 - 8(infrared-red)] \cdot 5 \} / 2
      Atmospherically resistant vegetation index (ARVI)
4.
             = (\rho^* \text{nir} - \rho^* \text{rb})/(\rho^* + \rho^* \text{rb})
                    where \rho^* rb = \rho^* r - \gamma (\rho^* b - \rho^* r).
                   \rho^* r =  ozone absorption and molecular scattering
      Modified soil and atmospherically resistant vegetation index
5.
      (MSARVI)
             =\{2\rho*nir + 1 - [2\rho*nir + 1)^2 - 8(\rho*nir - \rho*rb)]^{0.5}\}/2
6.
      Transformed vegetation index (TVI)
             = (ND7 + 0.5).5
             where
                      ND7 = (CH7-CH5)/(CH7+CH5)
      Modified TVI
7.
             = ((ND7+0.5)/ABS(ND7+0.5)) *(ABS(ND7+0.5).5
             where ND7 = (CH7-CH5)/(CH7+CH5)
8.
      Difference vegetation index (DVI)
             = 2.4CH7 - CH5
9.
      Ashburn vegetation index (AVI)
             = 2.0CH7 - CH5
      Tasseled Cap composed of 4 axes (Crist and Cicone, 1985)
10.
             = Soil brightness index, SBI (brightness)
             = Green vegetation index, GVI (greenness)
             = Yellow stuff, YVI
             = Nonsuch, NSI
```

(Adapted from Ashburn, 1978; Deering et al., 1975; Huete, 1994; Kanth and Thomas, 1976; Perry and Lautenschlager, 1984; Richardson and Weigand, 1977; Tucker, 1980)

Vegetation indices are sensitive to solar elevation angle, solar azimuth angle, and the look angle of the satellite platforms (Duggin, 1980; Kirchner and Schnetzler, 1981). An additional concern is the coordination of NDVI generated from different platforms and even the same platform at different times in its life cycle (Price, 1987). Performance of satellite components is subject to conditions present in orbit and the degradation of parts over repetitive usage. These slight variations are significant when compared to the amount of information within each pixel.

The evaluation of NDVI for finer-resolution satellites is limited by factors other than those of the NOAA series of satellites. Research into the local application of NDVI, generated by Landsat MSS and TM, and satellites with spatial resolution better than 30 m² has been directed toward the issue of noise. NDVI signals may be affected by atmospheric conditions or the presence of soil patches intermingled with ground cover within a pixel. Several modifications to the standard NDVI have attempted to compensate for these influences (Table 1.2). However, the question remains: to what extent does the topography affects influence a fine-resolution NDVI when it is applied to a localized area?

NDVI is a tool utilized to gather information about vegetation in a particular region. Information gathered is input into studies that examine global change (Baker et al., 1995; Overpeck et al., 1990). Proper interpretation of NDVI, at the global or regional scale of spatial resolution, is necessary for accurate understanding of change. Baker et al. (1995) looked to the sensitive forest-tundra ecotone as an indicator of global change. Understanding all sources

of noise within a fine-resolution NDVI signal is needed for accurate assessment of possible climate change as indicated by altering vegetation patterns in mountainous ecotones. Examination of the remaining topographic effect within NDVI is one such possible source of noise that needs to be investigated.

1.6 Research question

The importance of vegetation indices necessitates further research toward understanding those processes which affect the signal received and the information content derived. topography of a region, the atmosphere through which the signal must travel, and the spatial resolution of the satellite sensors all have an impact upon the information obtained. Although all are important areas of scientific inquiry, the scope of this study is focused on the examination of topographic influence for a single vegetation index, calculated for one time, under clear sky conditions, and in a mountainous terrain. Formally expressed, the research questions are: (1) Is NDVI sensitive to topographic effects?; and (2) How strong is the topographic "noise" relative to vegetation information ("signal") in the vegetation index image? In other words, are the influences that are acting upon NDVI values, for a mountainous terrain, solely related to vegetation or is there a topographic influence as well?

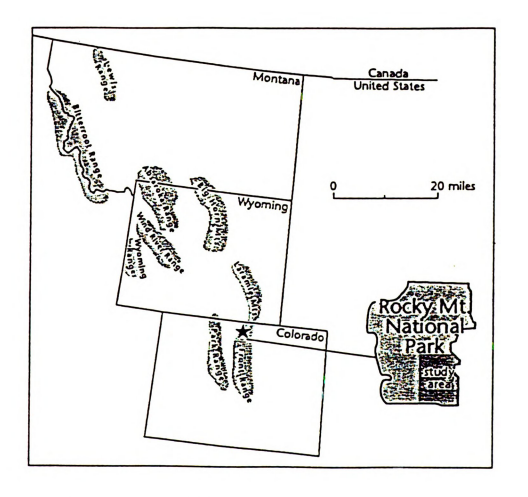
CHAPTER 2 SITE DESCRIPTION

2.1 Study area

Rocky Mountain National Park (RMNP) is located within the Colorado Front Range, northwest of Boulder, Colorado. This range extends for 300 km from the Arkansas river in the south into the state of Wyoming in the North(Peet, 1981). The study area is located within RMNP, 40° 10′ N to 40° 32′ N latitude and 105° 31′ to 105° 41′ west longitude (Peet, 1981). Specifically, the study site includes a 27,000 hectare portion of Southeast RMNP (Figure. 2.1).

RMNP straddles the Continental Divide. Elevations range from approximately 1830 m to roughly 4000 m. Much of the topographic variation seen today is due to the differential weathering of Pleistocene glaciated mountains (Allen et al., 1991). Richmond (1960) reports that the protection of the unspoiled examples of glaciation was a major impetus in the creation of RMNP. Underlying geology is mostly Precambrian granites, gneisses, and schists (Peet, 1981).

Vegetation within RMNP has been described in the context of life zones. A life zone attempts to organize vegetation within similar regions based on moisture, winds, exposure, and topography (Nelson, 1953). One classification includes: foothills, montane, subalpine, and alpine life zones (Peet, 1978b). One classification is based on climate conditions at increasing elevation (Veblen and Lorenz, 1991). Each zone contains characteristic vegetation that occurs due to climate conditions which are chiefly controlled by elevation and moisture (Peet, 1978a).



(Adapted from Brown, 1994.)

Figure 2.1. Study area within Rocky Mountain National Park.

Dominant vegetation types in Rocky Mountain National Park include: Aspen (Populus tremuloides), Douglas-Fir (Pseudosuga menziesii), Limber pine (Pinus flexilis), and Ponderosa pine (Pinus ponderosa) forests (Chiou and Hoffer, 1994). Other forest dominants include Blue Spruce and Subalpine Fir (Frank, 1988), Alder (Alnus spp.), and Lodgepole pine (Pinus contorta). Non-forest cover types include: alpine tundra, moist and dry meadows, bogs, rock outcrops, krummholz, ponds, willow, grasses, and sedges (Frank, 1988). Krummholz, a German word meaning twisted wood, identifies the dense, low mats of spruce and fir trees in the transition zone between forest and alpine tundra (Veblen and Lorenz, 1991).

Climatic conditions will vary both with elevation and latitude (Peet, 1978b). Vegetation response to climate conditions result in species gradation between successive zones of climate. For any particular species, the density and vigor of the individual examples varies with minor gradients of climate. A given species may appear on a variety of slopes and aspects. Appearance of a species will vary in density and size according to presence or lack of ideal conditions. These factors of topographic position and moisture availability are closely related to forest composition (Peet, 1978b). Limber pine, for example, occupies xeric sites between montane forest levels and treeline (Peet, 1978). Higher, rockier elevations within the park are most associated with the transition from forest to tundra. Within this region can be found species of spruce, fir, and occasionally Limber pine (Weisberg and Baker, 1995). Lower elevations (i.e., montane) support more mesic environments with

other conifer species such as Douglas fir and Ponderosa pine (Veblen and Lorenz, 1991). Variation within the general trend of deciduous to subalpine to alpine and tundra species of vegetation will be due to local conditions of climate. These variations include maximum height attainment for a species, density of a stand, and recovery from disturbances.

Remote sensing of the vegetation in RMNP is not new. Previous studies have utilized Landsat data, combined with a geographic information system (GIS) to analyze spatial patterns within RMNP (Baker and Weisberg 1995). The utilization of digital terrain information to complement the use of remote sensing and GIS is exemplified by Brown (1994). Landsat TM data was combined with topographic data to compare the relationship between vegetation and topography at the sensitive alpine treeline ecotone.

Analysis of vegetation through remote sensing serves both current research initiatives and practicality. Baker and Weisberg (1995) discuss the importance of understanding population parameters to further comprehend the dynamic environment in ecotones. Baker et al. (1995) connect changes in the forest tundra ecotone to global change. Determination of whether global change is altering mountain vegetation communities is a monumental task made more difficult by its remote physical environment. Remote sensing, GIS, and digital terrain data offer a practical means to understand vegetation communities in a terrain that is difficult to access.

CHAPTER 3 DATA AND METHODS

3.1 Addressing the Research Ouestion

This investigation will address the question of the degree to which vegetation and topography influence NDVI by separately modeling the influence of each factor using a remotely sensed satellite image, a vegetation map, and a digital elevation model (DEM). Topographic corrections have historically not been applied to the satellite radiance values prior to calculation of the index. This study will not stray from this precedent. The study is only plausible due to the existence of detailed groundcover data with which to compare and categorize the generated NDVI values. Again, the research question is: Are the influences that are acting upon NDVI values, for a mountainous terrain, solely related to vegetation or is there a topographic influence as well?

Homogeneous vegetation and topography classes were identified, using a digitized vegetation map and a DEM, respectively. NDVI values within these areas were compared to assess their influence. In previous studies, NDVI has been used as a surrogate for leaf area index and biomass based on an assumption that radiance is related to density and composition (Tucker, 1979). However, with the use of detailed ground cover data, I examined the possible influences of density and composition of vegetation and topography on NDVI.

3.2 Data

3.2.1 Landsat Thematic Mapper image

Radiance data for RMNP are provided in a Landsat 4 Thematic Mapper (TM) image (scene id # 425461765) acquired on July 5, 1989. Landsat TM provides ground resolution cells of 30 m x 30 m. Specifically, channels 3 and 4 (0.63 - 0.69 μ m and 0.76 - 0.90 μ m, respectively) were used to calculate NDVI (Tucker, 1979). Additional information about Landsat image channels may be found in Appendix A. The image was georeferenced to the UTM coordinate system, zone 13. The root mean square error (RMSE) for the rectification was less than 30 meters (R. Thomas, unpublished). RMSE is a measure of error between sample points in a rectified image and their known locations on the ground; it is the distance between input image control points and the same points after rectification (Erdas, 1991). The areal coverage (677 rows by 451 columns) was a subset from the original scene and ranges from (1061017 m, 405234 m) to (1051411 m, 394921 m) (Figure 2.1). Additional information about the Landsat image may be found in Appendix B.

The Landsat Thematic Mapper image (figure 3.1) of the test site was originally displayed using bands 4, 3, and 2 (display colors of red, green, and blue, respectively). Vegetation appears as shades of red because of the dominance of near-infrared (band 4) reflectance from vegetation.



Figure 3.1. Landsat TM image bands 4,3,2 displayed in RGB.

3.2.2 Digital elevation model (DEM)

A DEM for the RMNP study site was acquired from the United States Geological Survey (USGS), corresponding to 1:24,000 scale 7-1/2 minute topographic quadrangles (30 meter resolution). A previous study by Brown and Bara (1994) has shown systematic biases (striping) present in DEMs generated by photogrammetric means. The production of DEMs involves the use of photographic scanners and manual profiling which produce "striping" features in the final product. A 1-by-3 filter was used to reduce the striping effect present in the data (Brown and Bara, 1994). The vertical accuracy of the DEM is reported at +/- 7 meters (USGS, 1987).

3.2.3 Vegetation cover map

A detailed, digital vegetation map for Rocky Mountain

National Park was created by park conservation personnel and field checked by Karl Hess (Colorado State University). Nine dominant forest types and sixteen non-forest vegetation classes were surveyed (Table 3.1). Forest types were broken down into multiple sub-classes to include density data. In addition, the locations of krummholz and rock outcrops were recorded where present.

Additional modifiers to vegetation classes included information on disease, mountain beetle damage, disturbance, and rock outcrops. A total of 409 different classes of vegetation was identified and mapped. Landcover changes are assumed to be negligible for the one year time duration between map creation and image capture.

Table 3.1. Original groundcover classifications for Rocky Mountain National Park.

Forest Types	Size Classes	Density
Aspen	0" - 5"	0 - 20%
Douglas Fir	5" - 10"	20 - 40%
Limber Pine	10" -15"	40 - 60%
Lodgepole Pine	15" - 20"	60 - 80%
Ponderosa Pine	20" +	80 - 100%
Spruce/Fir		

Other Types

Alder/Aspen

Bog

Cottonwood*

Wet meadow

Open water/pond

Blue Spruce*

Rushes/cattail

Willow

Non-Vegetated	Dry Meadow
Disturbed/artificial	Grass/forb
Rock	Shrub/sage
Sandbar	•

Alpine

Grass/forb Willow

Modifications to the above classes:

disturbed, mountain beetle killed, krummholz, rock outcrop

* includes density and Diameter at Breast Height (DBH) data

3.3 Preparing the data

3.3.1 Generating NDVI

Digital numbers (DN) of the Landsat TM bands were first converted to radiance values for this investigation. The use of radiance data is but one of several cautions necessary when manipulating satellite imagery for analysis of vegetation indices. Digital numbers are the nominally-scaled amplitudes of radiance measured at each of the satellite's sensors and must be corrected for slight imbalances between each of the detectors in order to calculate radiance (EOSAT, 1994). The use of DNs is deemed inappropriate for NDVI calculations due to the index's sensitivity to intensity of irradiance and reflected radiance (Goward et al., 1993).

Other cautions are raised when comparing calculated NDVI between sensors and between platforms. Any comparison of NDVI between sensors or platforms should only be conducted with full knowledge of the calibration procedures of each (Goward et al., 1991). These cautions may seem to place extreme limitations on a NDVI study of TM generated values. However, due to the nature of this investigation, such cautions will not serve to limit the scientific findings for two reasons. The first is that many of the above cautions were based on findings of NDVI generated from Advanced Very High Resolution Radiometer (AVHRR) data. This sensor has a much larger field-of-view and, hence, much coarser spatial resolution than the Landsat TM (Goward et al., 1991). By using one Landsat image, assumptions of nadir (i.e., vertical) satellite position may be made for all elements being investigated (i.e., pixels). Secondly, this investigation does not include a comparison between

different sensors of the same satellite type nor is it a comparison of NDVI generated from different platforms.

The objective is to investigate the possible systematic influences of vegetation cover and topography on NDVI. The combination of detailed ground data, a DEM, and a Landsat TM image, converted to radiance values, enabled this investigation to proceed without concern for many of the limitations cited in other applications of NDVI (Goward et al., 1991; Guttman, 1993; Perry, 1984; Price, 1987). Conversion of DNs to radiometric units facilitates the accurate computation of NDVI (Price, 1987). The general equation for the conversion of digital numbers is:

DN'= Int[((DN-DNmin $_{\lambda}$)/(DNmax $_{\lambda}$ -DNmin $_{\lambda}$))*(max $_{\lambda}$ -min $_{\lambda}$)+min $_{\lambda}$] (3.1) Where:

DN = digital number for an individual pixel, DN' = recalculated digital numbers, $DNmin_{\lambda} = \text{minimum digital number in wavelength } \lambda,$ $DNmax_{\lambda} = \text{maximum digital number in wavelength } \lambda,$ $min_{\lambda} = \text{minimum radiance value recorded in wavelength } \lambda,$ $max_{\lambda} = \text{maximum radiance value recorded in wavelength } \lambda.$

Each transformation is wavelength band specific, although the recalculated range of values (converted to integer range of 0 - 255) is based on the maximum range from both bands.

Numbers generated from the Landsat DN to radiance transformation (Equation 3.1) were scaled to an integer range of 0-255 for use in a geographic information system (GIS). The end

result of this calculation is the elimination of the slight miscalibrations of radiance measurements in each of the independent sensors (EOSAT NOTES, 1994). Raw radiance values, used for the calculation of NDVI, were adjusted only in scale to accommodate analysis within an integer-only framework. Each pixel was transformed using the ALGEBRA program within the ERDAS image analysis software package.

Once rescaled to the same range of radiance, these two image bands were then combined algebraically to create the NDVI index (Figure 3.2). Lighter areas indicate a greater amount of vegetation (i.e., photosynthetically active radiation, biomass, LAI, etc.) than areas with darker shading. The influence of topography on NDVI response is apparent. Lighter shades in the NDVI image tend to correspond to the valley locations, whereas the ridge (i.e., higher elevation) sites tend to have lower NDVI values.



Figure 3.2. NDVI image generated from radiance values.

3.3.2 Calculating incidence angle

Irradiance, a measurement of available incident radiation for any given location on the ground, may be used to determine the extent of the topographic effect on NDVI. However, the term irradiance implies that atmospheric conditions are known and incorporated in its calculation. In this investigation, these atmospheric conditions were assumed to be uniform due to limited satellite scene size and clear sky conditions. Under clear sky conditions, variability of incoming solar radiation is dominated by direct irradiance (Dubayah and Rich, 1995). In place of the irradiance measure, incidence angle will be used. Cosine of the incidence angle, i, is a measure of direct illumination as a function of topographic position and is determined by the slope angle and aspect at each pixel (Figure 3.3). It is the angle between the normal to any given point and the direct path rays of the sun (measured in degrees above the horizon and compass direction).

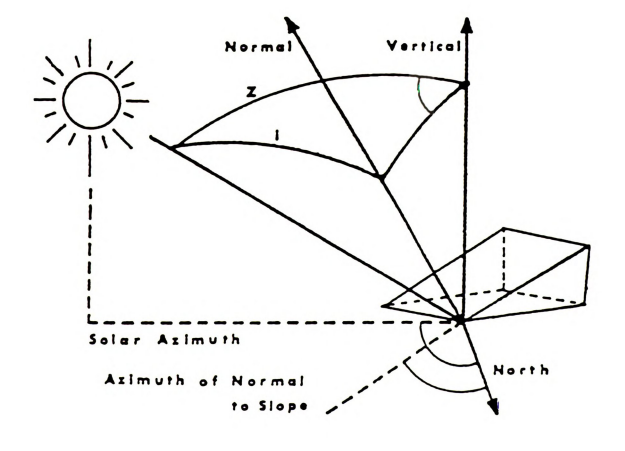


Figure 3.3. Solar incidence angle, i. (Reprinted from Teillet et al., 1982).

Other influences upon incoming solar radiation are diffuse sky irradiance and reflected radiance, both direct and diffuse, from nearby terrain (Dubayah and Rich, 1995; Proy et al., 1989; Woodham and Lee, 1985). These additional influences on radiation at the earth's surface are important, but not as influential as the solar illumination angle. The simple application of mere solar illumination to create radiation maps can only be accurate under clear-sky conditions (Dubayah and Rich, 1995). Under any other conditions, the radiation measurement must be augmented by additional considerations of diffuse sky and reflected radiance within a mountainous region. Again, for simplicity, the incident radiation upon the topographic data were represented in cos(i) form.

A map of cos(i) was first calculated using the DEM and information about the sun's location at the time of image capture. The incidence angle map was generated using the HILLSHADE command in Arc/Info, without the shadow option (Equation 3.2):

```
\cos(i) = 255 \left[\cos(S) \sin(s) \cos(a-A) + \sin(S) \cos(s)\right] 
where:
```

s = terrain slope angle (calculated from DEM),

S = solar zenith angle (30°),

 $S = 90^{\circ}$ - solar elevation (60°),

a = terrain slope aspect (calculated from DEM),

A = solar azimuth angle (118*).

Sun and sensor angles, necessary to calculate the incidence angle map, were obtained from header information of the Landsat 4 seven band digital data.

The measure of incidence angle for each pixel is a variation of a shaded relief map generated with the sun elevation and azimuth positions corresponding to the time of satellite image capture. Figure 3.4 is the $\cos(i)$ map utilized in this study.

The measure of incidence angle for each pixel is a variation of a shaded relief map generated with the sun elevation and azimuth positions corresponding to the time of satellite image capture. Figure 3.4 is the $\cos(i)$ map utilized in this study.



Figure 3.4. Map of cos(i).

3.3.3 Shadow map

The calculation of the incidence angle map (Figure 3.4)does not include the effect of shadows. A shadow is caused when surrounding landforms completely block direct radiation from the sun. A map of shadows was calculated from the DEM using sun angles at the time of image capture. Each pixel of the DEM is compared to its neighbors and the angle of direct sunlight (Dubayah and Rich, 1995). Again, the command HILLSHADE was used in Arc/Info to generate the shadow map. Pixels in shadow (a total of 33) were removed from further analysis.

3.3.4 Vegetation reclassification

In order to examine the relationships between vegetation type and NDVI, the 409 cover type classes from the vegetation map of RMNP were reclassified into groups of similar expected NDVI Nineteen cover classes were formed by combining classes according to similar ground cover types. For several of the forest cover classes, density data and information on the presence of krummholz and rock outcrops were detailed and used as discriminating factors. Density classes of 0-20%, 20-40%, 40-60%, 60-80%, 80-100% were included for classes dominated by Douglas Fir, Aspen, Limber Pine, Lodgepole Pine, Ponderosa Pine, Spruce/Fir, and Blue Spruce. Eleven other classes of vegetation cover, forest and non-forest categories, were included but were not augmented by density data. Two classifications, one based on density and the other on dominant vegetation type were cross-tabulated to produce a total of 210 possible classes. Classes of dominant vegetation are listed in Table 3.2, and density classes in Table 3.3.

Table 3.2. Vegetation cover classes.

Class #	Classification
0.	Other
1.	Open water
2.	Non-vegetated
3.	Alpine
4.	Dry meadow
5.	Bog, wet meadow
6.	Combinations of Lodgepole, Limber Pine, and
	Spruce/Fir with the presence of krummholz
7.	Combinations of Lodgepole, Limber Pine, and
	Spruce/Fir without the presence of krummholz
8.	Other combinations of conifers
9.	Combinations of Ponderosa Pine and Douglas Fir
10.	Blue Spruce
11.	Mixtures of deciduous and conifer species
12.	Combinations of Willow, Aspen, and Alder
13.	Combinations of conifer forest with wet meadow
14.	Combinations of deciduous forest with dry meadow
15.	Empty classification
16.	Alpine grass and willow appearing with rock outcrops
17.	Combinations of Lodgepole, Limber Pine, and
	Spruce/Fir with the presence of rock outcrops
18.	Ponderosa Pine
19.	Ponderosa Pine with presence of rock outcrops
20.	Alpine species of grass and willow appearing with wet meadow

Table 3.3. Forest density classifications.

Class	Density
1.	0-20%
2.	0-20% with rock
3.	20-40%
4.	20-40% with rock
5.	40-60%
6.	40-60% with rock
7.	60-80%
8.	60-80% with rock
9.	80-100%

Of the 210 possible combinations of classes, only 39 were shown to have actual representation on the ground. The list of these classes may be found in Table 3.4. Several classes were combined due to similarity of NDVI means, low standard deviations, and similarity of vegetation. The final classification is listed in Table 3.5.

Figure 3.5 depicts the final 33-class vegetation classification. Notice that classes 7, 9, 11, 13, and 15 (i.e., combinations of Limber pine, Lodgepole pine, Spruce fir, krummholz, and rock outcrops) are the dominant forest types within this region. Therefore, the areal extents of these classes is noticeably larger than the others.

Table 3.4. Reclassified cover classes from original vegetation map.

Class	Description	-	NDYI	SID
0.	Other	1831		13.0
1.	Non-vegetated, no density data	10270		12.1
2.	Alpine, no density data	2191	81.6	10.6
3.	Alpine, 80 - 100%	232	80.5	13.8
4.	Dry meadow, 80 -100%	65	89.3	11.22
5.	Bog, wet meadow, rushes, cattails, no density data	160	89	10.0
6.	Bog, wet meadow, rushes, cattails, 80 -100%	5 9	91	14.2
7.	Lodge Pole Pine, Limber Pine, Spruce Fir,			
	with presence of krummholz, 0 - 20%	8 2	84.1	9.8
8.	Lodge Pole Pine, Limber Pine, Spruce Fir,			
	with presence of krummholz, 20 - 40%	28	86.6	7.1
9.	Lodge Pole Pine, Limber Pine, Spruce Fir, with			
	presence of krummholz, 20 - 40% & rock outcrops	1 2	90.1	5.1
10.	Lodge Pole Pine, Limber Pine, Spruce Fir, with			
	presence of krummholz, 40 - 60%	685	83.7	10.6
11.	Lodge Pole Pine, Limber Pine, Spruce Fir, with			
	presence of krummholz, 60 - 80%	169	85.0	10.7
12.	Lodge Pole Pine, Limber Pine, Spruce Fir, 0 - 20%	190	85.2	9.7
13.	Lodge Pole Pine, Limber Pine, Spruce Fir, 20 - 40%	296	85.4	10.2
14.	Lodge Pole Pine, Limber Pine, Spruce Fir, 20 - 40%,			
	with presence of rock outcrops	4	84.0	1.9
15.	Lodge Pole Pine, Limber Pine, Spruce Fir, 40 - 60%	880	86.4	8.3
16.	Lodge Pole Pine, Limber Pine, Spruce Fir, 40 - 60%,			
	with presence of rock outcrops	119	83.8	14.4
17.	Lodge Pole Pine, Limber Pine, Spruce Fir, 60 - 80%	1776	87.1	7.6
18.	Loge Pole Pine, Limber Pine, Spruce Fir, 60 - 80%,			
	with presence of rock outcrops	194	80.9	11.4
19.	Lodge Pole Pine, Limber Pine, Spruce Fir, 80 - 100%		86.6	7.8
20.	Other conifer mixtures, 0 - 20%	28	85.4	11.5
21.	Other conifer mixtures, 0 - 20%, rock outcrops	56	93.0	7.6
22.	Other conifer mixtures, 20 - 40%, rock outcrops	2	85.7	2.6
23.	Other conifer mixtures, 40 - 60%	10	71.0	5.4
24.	Other conifer mixtures, 40 - 60%, rock outcrops	8	84.5	2.0
25.	Ponderosa Pine, Douglas Fir, 20 -40%	6	98.0	10.2
26.	Ponderosa Pine, Douglas Fir, 40 -60%,	4	77.6	16.6
27.	Blue Spruce, 0 - 20%	1	92.3	
28.	Blue Spruce, 40 - 60%	1 4	67.3	9.3
29.	Blue Spruce, 60 - 80%	6	92.4	9.4
30.	Deciduous, conifer mixture, 0 - 20%	16	89.0	3.9
31.	Deciduous, conifer mixture, 40 - 60%	4	80.6	6.2
32.	Deciduous, conifer mixture, 80 - 100%	100	95.9	11.3
33.	Willow, Aspen, Alder, 0 - 20%	19	83.7	4.7
34.	Willow, Aspen, Alder, 40 - 60%	142	86.7	7.0
35.	Willow, Aspen, Alder, 60 - 80%	18	91.2	7.2
36.	Willow, Aspen, Alder, 80 - 100%	1 1	87.4	3.9
37.	Forest, wet meadow, conifer	15	79.3	8.2
38.	Alpine with presence of rock, no density data	1301	77.0	11.4
39 .	Alpine, wet meadow, no density data	100	92.0	7.8

Table 3.5. Final classifications of composition/density classes.

Class	# Vegetation/density cover class	Sk Area (ha) Fao	
0.	Other	12100	50
1.	Alpine	2423	25
2.	Dry meadow	65	4
3.	Bog, wet meadow, rushes, cattail, and no data	218	5
4.	Lodge Pole Pine, Limber Pine, Spruce Fir, Krummholz, 0-20%	82	5
5.	Lodge Pole Pine, Limber Pine, Spruce Fir, Krummholz, 20-40%	28	3
6.	Lodge Pole Pine, Limber Pine, Spruce Fir, Krummholz, 20-40% + rocks	12	2
7. 8.	Lodge Pole & Limber Pines, Spruce Fir, Krummholz, 40-60%	685	15
o. 9.	Lodge Pole & Limber Pines, Spruce Fir, Krummholz, 60-80% Lodge Pole & Limber Pines, Spruce Fir, Krummholz,	169	5
<i>J</i> .	0-40%	486	10
10.	Lodge Pole Pine, Limber Pine, Spruce Fir,		- •
	20-40% + rocks	4	1
11.	Lodge Pole Pine, Limber Pine, Spruce Fir, 40-60%	880	20
12.	Lodge Pole Pine, Limber Pine, Spruce Fir, 40-60%		
	40-60%+ rocks	119	4
13.	Lodge Pole Pine, Limber Pine, Spruce Fir, 60-80%	1776	20
14.	Lodge Pole Pine, Limber Pine, Spruce Fir, 60-80% + rocks	194	5
15.	Lodge Pole Pine, Limber Pine, Spruce Fir, 80-100%	6380	25
16.	Other conifer mixtures, 0-20%	28	3
17.	Other conifer mixtures, 0-20% + rocks	56	4
19.	Other conifer mixtures, 40-60%	10	2
20.	Other conifer mixtures, 40-60% + rocks	8	1
21.	Ponderosa Pine, Douglas Fir, 20-40%	6	i
22.	Ponderosa Pine, Douglas Fir, 40-60%	4	i
24.	Blue Spruce, 40-60%	14	2
25.	Blue Spruce, 60-80%	6	1
26.	Deciduous, Conifer mixture, 0-20%	16	2
27.	Deciduous, Conifer mixture, 40-60%	4	1
28.	Deciduous, Conifer mixture, 80-100%	100	
29.	Willow, Aspen, Alder, 0-20%	19	5 2 5 2
30.	Willow, Aspen, Alder, 40-60%	142	5
31.	Willow, Aspen, Alder, 60-80%	18	
32 .	Willow, Aspen, Alder, 80-100%	11	1
33.	Forest, Wet meadow, Conifer, 60-80%	15	2
34.	Alpine, without density data with rock	1301	20
35.	Alpine, Wet meadow, no density data	100	5

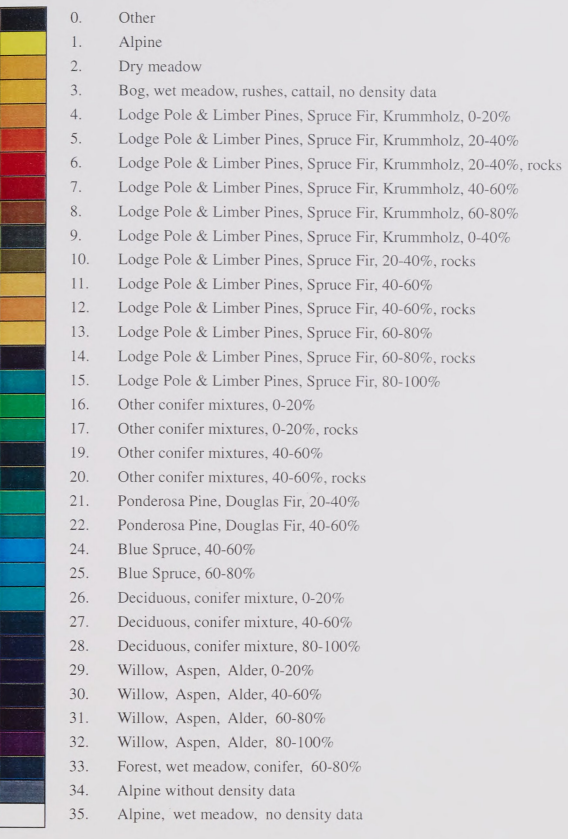


Figure 3.5. Vegetation/density classification map legend.



Figure 3.5 (Cont'd).

3.3.5 Raw and classed cos(i) (incidence angle)

Cos(i) data were incorporated into the analysis in two forms: (1) as a raw measure of illumination for each pixel location and (2) as classed groups of similar cos(i). The ways in which the two forms of incidence angle were used in the analysis are discussed in the statistical techniques section of this chapter. The raw cos(i) values were calculated using Equation 3.2 and the ALGEBRA program of ERDAS.

The classification of $\cos(i)$ is a compromise between equal area and equal interval approaches to classification. A histogram of the incidence angle revealed a large number of pixels with values greater than $\cos(i) = 0.6$. A cut-off at $\cos(i) = 0.6$ was used as the upper limit of the first class of $\cos(i)$. The remaining four classes divided the range of 0.6 - 1.0 into four equal intervals. The resulting classification is listed in Table 3.6.

Table 3.6. Classification of cos(i), range 0-1.

Class	$\cos(i)$	Area (ha)
1.	< 0.6	3348
2.	0.6 - 0.7	3135
3.	0.7 - 0.8	5966
4.	0.809	8807
5.	0.9 - 1.0	6223

3.4 Methods

3.4.1 Sampling the Data

In a final preparation step, data on plant cover and incidence angle, masked for shadows, were combined with a map of NDVI in order to address the research questions. A program in the ERDAS image analysis software package was used to generate samples of pixels for NDVI, vegetation class, incidence angle, and incidence angle class.

The pixel values for each of the variables are highly correlated to those areas (pixels) immediately surrounding it (apparent in their non-random patterns in Figures 4.1, 4.3, and 4.5). This spatial autocorrelation is reduced with increased distance away from the original pixel. To alleviate the potential biasing of statistical tests associated with this phenomenon, a stratified, systematic sampling was adopted. Pixels were sampled at regular pixel intervals in the x and y directions using the following skip factors: 50, 20, 15, 10, 5, 4, 3, 2, 1. The skip factor used for each class was set according to the largest interval that yielded approximately 30 samples, a minimum value necessary for statistical analysis. Many of the smaller classes required a very small skip factor and even no skip factor at all (Table 3.5). The adopted approach allowed for a reduction of the effects of spatial autocorrelation to the maximum extent possible while including as many classes as possible.

3.4.2 Statistical techniques

A combination of bivariate regression and analysis of variance (ANOVA) statistical tests were performed to evaluate the hypothesized relationships. Again, the research question: Are the influences that were acting upon NDVI values, for a mountainous terrain, solely related to vegetation or is there a topographic influence as well? ANOVA tests were employed to determine if sample groups of NDVI had significant differences. Bivariate regressions were used to test the expected relationship between NDVI and each of the variables tested. Results of these regressions address the more specific question: "Of what form is the relationship?" The strengths of the relationships were tested for statistical significance.

Two groups of statistical tests were employed, one based on classes of pixels by vegetation type and the second by incidence angle class. Each group of statistical tests involved two steps. In the first step, ANOVA statistical tests were conducted to examine the similarity or difference of NDVI values by class. The first group of statistical tests focused on the differences in NDVI for the 33 classes of vegetation/density. The second group of statistical tests was directed at the differences in NDVI for classes of similar incidence angle. In the second step, within each classification (i.e., by vegetation type and incidence class) the influence of the other variable on NDVI was assessed using either bivariate regression (in the case of incidence angle) or ANOVA (in the case of vegetation class).

The first group of tests was based on vegetation type classes.

ANOVA was employed to test the differences within and between groups. The ANOVA test determined whether the groups of vegetation have significantly different NDVI values.

 H_0 : $\mu_1 = \mu_2 = \mu_3 = ... = \mu_{35}$ The samples of NDVI for each vegetation class are drawn from the same population

H_a: $\mu_1 \Leftrightarrow \mu_2 \Leftrightarrow \mu_3 \Leftrightarrow ... \Leftrightarrow \mu_{35}$ At least one sample is drawn from a different population

Should the null hypothesis be rejected, signifying that at least one sample is drawn from a different population, then it can be concluded that NDVI is related to vegetation type.

The influence of incidence angle on NDVI for groups of similar vegetation was then evaluated using bivariate regression. NDVI values were extracted by the 33 vegetation/density classes. Within each of the classes of vegetation, NDVI values were regressed with values of incidence angle, $\cos(i)$.

Regression for vegetation groups 1-35: NDVI = a + b[cos(i)]

H_O: b = 0; There is no relationship between NDVI and incidence angle for pixels in this vegetation class.

H_a: b <> 0; A relationship exists between NDVI and incidence angle for pixels in this vegetation class.

This statistical test aided in the determination of whether or not NDVI is affected by incidence angle, how strong the relationship is, and the direction of the relationship. These tests were performed while controlling for the influence of vegetation type, because vegetation type and incidence angle may be interrelated.

The second group of statistical tests was based on incidence angle classes. Groups of incidence angle were reclassified to five ranked classes (Table 3.6). ANOVA was employed to test the differences within and between groups.

Ho: $\mu_1 = \mu_2 = \mu_3 = \mu_4 = \mu_5$ The samples of NDVI for each incidenceangle class are drawn from the population

Ha: $\mu_1 \Leftrightarrow \mu_2 \Leftrightarrow \mu_3 \Leftrightarrow \mu_4 \Leftrightarrow \mu_5$ At least one sample is drawn from a different population

Should the null hypothesis be rejected, then it could be said that incidence angle accounts for some of the variability of NDVI. This information alone is not complete, because, although incidence angle may influence NDVI measurements directly, it also may be related to NDVI indirectly by affecting vegetation patterns. Brown (1994) showed that vegetation patterns are sensitive to levels of exposure to solar radiation.

Next, from the vegetation classification, each class of vegetation was revalued to take on its average NDVI value (i.e., its expected NDVI). This expected NDVI (NDVI_e) was to be regressed against actual NDVI values, for each incidence angle class, to

discover influences of vegetation on groups of similar incidence angle.

Planned regression for incidence angle groups 1-5 NDVI_e vs. NDVI For each ranked incidence group:

$$NDVI = a + b(NDVI_e)$$

Ho: b = 0; There is no relationship between predicted NDVI, for this class of incidence angle, and actual NDVI.

Ha: b <> 0; A relationship exists between expected NDVI, for this class of incidence angle, and actual NDVI.

This statistical test was to aid in the determination of whether or not the NDVI values for groups of similar incidence angles are related to vegetation.

With incidence angle held constant, the relationship between vegetation type and NDVI could not be tested with bivariate regression. Too few vegetation classes per incidence class (Table 3.7) did not provide enough different NDVI_e values to run the bivariate regression. The analysis was, therefore, not conducted.

Table 3.7. Vegetation class occurrence within incidence classes.

Vegetation Class	1	Incide 2	nce (Class 4	5	Total
0.	9	6	6	9	16	46
1.	6	4	11	17	2	40
2.	Ŏ	Ö		29	14	46
3.	Ö	3	3	78	8	92
4.	Ō	Ō	40	10	20	34
5	0	0	10	14	16	31
6.	0	0	0	21	14	35
7.	1		6	11	13	33
8.	0	2 3	16	20	30	69
9.	0	4	12	14	17	47
10.	0	3	35	2	0	40
11.	3	2	6	6	9	26
12.	20	4	8	20	33	85
13.	0	6	8	16	11	41
14.	15	25	22	17	8	87
15.	5	8	25	41	17	96
16.	0	0	0	22	13	35
17.	0	5	11	12	14	42
19.	17	10	0	3	0	30
20.	0	11	75	1	0	87
21.	0	0	0	0	63	63
22.	0	0	0	28	9	37
24.	0	0	1	14	19	34
25.	0	7	18	22	14	61
26.	0	0	9	29	2	40
27.	0	0	3	34	1	38
28.	0	0	0	5	37	42
29.	9	15	26	0	0	50
30.	1	12	17	24	6	60
31.	0	69	0	22	20	111
32.	0	0	23	16	13	52
33.	33	0	25	0	15	73
34.	0	5	8	17	7	37
35.	0	1	18	22	2	43
totals	119	205	400	596	463	1783

CHAPTER 4

4.1 Statistical results

Table 4.1 depicts the ANOVA results for the two groups of classed pixels (i.e., by vegetation type and incidence class). These tests were utilized to determine whether significant relationships existed between NDVI and the tested variables of vegetation and incidence class. Specifically, (1) is NDVI related to vegetation type? and (2) is NDVI related to incidence angle?

Within each group of statistical tests, the ANOVA test was applied to two different sets of pixels. The first group included all sample pixels, regardless of skip factor. In the presence of spatial autocorrelation, statistical tests are more likely to yield significant results than when spatial autocorrelation is controlled. Therefore the second group utilized only those pixels sampled with a skip factor of ≥ 10. This second test examined the ANOVA relationship on those pixels that were sampled in a manner that limited the effects of spatial autocorrelation. The results indicate that, in each case, NDVI is significantly (p < 0.05) related to vegetation class and incidence angle class.

These initial ANOVA tests are not without their potential for misinterpretation. The relationships being reported, for groups of similar vegetation class and incidence angle, may potentially be the same interrelationship. To avoid misinterpretation, one variable must be held constant while the other is tested. Bivariate regressions were conducted to test the strength and directionality of the relationships between NDVI and the tested variables of

Table 4.1. ANOVA results for vegetation and incidence angle groups.

ANOVA A: Grouped by vegetation/density class

1. All sample pixels, outliers removed

 $Chi^2 = 540.075$ DF = 33 p = 0.00

source	sum-of-squares	DF	mean-square	F-ratio	р
between groups	67394.311	33	2042.252	34.411	0
within groups	101428.523	1709	59.350		

2. Sample pixels of with skip factor ≥ 10 (0, 1, 7, 9, 11, 15, 34).

 $Chi^2 = 49.687$ DF = 7 p = 0.00

source	sum-of-squares	DF	mean-square	F-ratio	р
between groups	12373	7	1767.573	23.621	0
within groups	26939.271	360	74.831		

ANOVA B: Grouped by incidence class

1. All sample pixels, outliers removed

 $Chi^2 = 90.724$ DF = 4 p = 0.00

source	sum-of-squares	DF	mean-square	F-ratio	р
between groups	16394.993	4	4098.748	46.734	Ō
within groups	152427.841	1738	87.703		

2. Sample pixels with skip factor ≥ 10 (0, 1, 7, 9, 11, 15, 34).

 $Chi^2 = 15.836$ DF = 4 p = 0.003

source	sum-of-squares	DF	mean-square	F-ratio	p
between groups	2164.932	4	541.233	5.289	Ō
within groups	37147.343	363	102.234		

vegetation type and incidence angle. NDVI values were regressed against corresponding raw cos(i) values for the samples within each vegetation/density class. Table 4.2 lists the number of samples, (x,y) skip factor, r^2 , f-ratio, p values, and the regression line coefficients for each regression of vegetation class.

With vegetation held constant, a relationship between incidence angle and NDVI was significant if it had a low p value (p<.05). The direction of the relationship (i.e., whether NDVI increases or decreases with any increase in incidence angle) is given by the sign (+ or -) on the regression coefficient (b) for incidence. The value of r^2 is a measure of how strong the entire relationship is between NDVI and incidence angle. Larger r^2 values indicate that more of the variation in NDVI is explained incidence angle. The label n indicates the number of samples used for that regression.

A large skip factor present in a vegetation class indicated that the vegetation class was sampled in a way that limited the effect of spatial autocorrelation. The larger the skip factor, the more the effect was limited. A vegetation class with a skip factor of 10 or greater may be interpreted with more reliability than one with a low skip factor (i.e., 5 or less). Four of these vegetation classes had significant relationships between incidence angle and NDVI:

Class #7 (p =0.011) Lodge pole & Limber pines, Spruce Fir, krummholz, 40-60%,

Class #9 (p =0.005) Lodge pole & Limber pines, Spruce Fir, krummholz, 0-40%, Class #11 (p =0.001) Lodge pole & Limber pines, Spruce Fir, 40-60%, and Class #15 (p =0.001) Lodge pole & Limber pines, Spruce Fir, 80-100%.

Table 4.2. Regression results for final 33 vegetation/density classes.

		skip				constant	incidence
Class	n_	factor	<u>r 2</u>	F-Ratio	<u>p</u>	(a)	(p)
0.	46	50	0.078	3.704	0.061	57.507	+0.071
1	40	25	0	0.012	0.914	84.425	-0.006
2.	46	4	0.149	7.698	0.008	37.771	+0.242
3.	89	5	0.032	2.875	0.094	55.669	+0.164
4.	28	5	0.088	2.515	0.125	99.34	-0.072
5.	31	3 2	0.061	1.882	0.181	107.094	-0.087
6.	35		0	0.012	0.913	87.264	+0.012
7.	33	15	0.191	7.309	0.011	57.7	+0.131
8.	69	5	0.008	0.551	0.461	80.761	+0.033
9.	47	10	0.163	8.752	0.005	57.901	+0.131
10.	39	1	0.06	2.358	0.133	94.687	-0.058
11.	27	20	0.388	15.878	0.001	68.53	+0.086
12.	85	4	0.333	41.399	0	62.474	+0.116
13.	41	20	0.049	2.06	0.165	75.697	+0.058
14.	87	5	0.001	0.109	0.742	78.586	+0.012
15.	96	25	0.061	6.94	0.015	76.284	+0.053
16.	35	3	0.056	1.944	0.173	127.129	-0.175
17	42	4	0.001	0.034	0.855	92.332	+0.007
19.	30	2	0.019	0.537	0.47	75.659	-0.029
20.	87	1	0	0.022	0.882	83.784	+0.004
21.	63	1	0.363	34.777	0	-194.93	+1.186
22.	37	1	0.013	0.444	0.509	32.774	+0.212
24.	34	2	0.002	0.049	0.826	76.377	-0.029
25.	61	1	0.31	26.446	0	51.6	+0.2
26.	40	2	0.093	3.902	0.056	71.04	+0.086
27.	38	1	0.031	1.144	0.292	112.90	1-0.149
28.	42	5	0.057	2.42	0.128	37.663	+0.238
29.	49	2	0.255	16.08	0	67.843	+0.095
30.	61	5	0.135	9.202	0.004	66.869	+0.1
31.	42	5 2	0.386	25.128	0	-21.806	+0.494
32.	121	1	0.125	16.957	Ö	77.06	+0.054
33.	41	2	0.609	60.641	Ö	25.753	+0.245
34.	38	20	0.003	1.798	0.188	97.106	-0.107
3 5 .	43	5	0.048	0.047	0.188	95.546	-0.107
JJ.	73	J	0.001	0.04/	0.029	73.340	-0.01/

These 4 classes are variations of one of the dominant vegetation types within the study site. Large areal extent of vegetation cover (i.e., large enough to allow sampling that limits the effect of spatial autocorrelation) may limit the applicability of a vegetation type/density combination for investigation. Discussion of the results and conclusions of the ANOVA and bivariate regressions are presented in Chapter 5.

CHAPTER 5 DISCUSSION AND CONCLUSIONS

5.1 Discussion

Incidence angle influence on NDVI measurements for vegetation classes was determined through (a) ANOVA based on classified incidence values and (b) bivariate regression of NDVI versus incidence angle for vegetation classes. ANOVA tests were conducted for NDVI values within and between each of the vegetation classes and for NDVI values between each of the classes of incidence (Table 4.1). ANOVA tests were tabulated for all pixel samples and for pixels from vegetation groups with skip factors ≥ 10.

Results from each group of tests showed that by increasing the skip factor to partially compensate for spatial autocorrelation, fratios and chi-squared values decreased. The relationship of incidence angle and NDVI are only reliable for those vegetation classes whose sampling skip factors partially compensated for spatial autocorrelation.

ANOVA results indicated a significant relationship between NDVI and vegetation type (p=0). Also indicated was the presence of a significant relationship between NDVI and incidence class (p= 0.003). The NDVI relationship was stronger with vegetation class (F= 23.62) than with incidence angle (F=5.29). However, the relationships between NDVI and incidence class were affected by the possibility that incidence angle may have influenced vegetation type. The variables were then examined independently.

When vegetation was held constant, incidence angle was shown to have an influence on the signal of NDVI. In all cases, the r² values for each of the 33 vegetation/density classes were low (ranging from zero to 0.61). Only 13 of the 33 regressions, by vegetation class were significant. In each case the relationship was positive, meaning that an increase in incident angle tended to correspond with an increase in NDVI. Of the 13 significant regressions, only 4 proved significant while also having a skip factor ≥ 10 pixels. R² values for these regressions suggested that incidence angle influenced as much as 39% of the variation in NDVI. Relationships of the vegetation classes, having significance but not large skip factors, were not considered because spatial autocorrelation in the samples can artificially inflate the significance values.

As skip factor decreased within the vegetation classes, a greater number of significant regression relationships between incidence and NDVI appeared. The observation indicated the importance of including skip factor as a means to limit the impacts of spatial autocorrelation present. Only 4 regressions had significance and skip factors ≥ 10 . These four were:

Class #7 Lodgepole & Limber Pine, Spruce Fir, and Krummholz, 40-60%;
Class #9 Lodgepole & Limber Pine, Spruce Fir, and Krummholz, 0-40%;
Class #11 Lodgepole & Limber Pine, Spruce Fir, without Krummholz, 40-60%;
Class #15 Lodgepole & Limber Pine, Spruce Fir, without Krummholz, 80100%.

These results indicated, at least for the four significant classes at skip factors of ≥ 10 , that incidence accounts for some noise

associated with the NDVI signal. The observation that the four vegetation classes came from the same dominant mix of vegetation should not be overlooked. These classes cover large areal extents and appeared under different topographic conditions (Table 4.3). Neither the presence of krummholz nor the density of the vegetation class appear to have much importance on incidence affecting NDVI. However, these observations were limited to the four significant relationships. The factor that may have influenced these observations is areal extent and whether the skip factor was large enough to compensate for autocorrelation. This limitation may have been the reason that some other classifications were not significant. It may also have limited the implications of this study; because only large extents of similar vegetation were sampled at a skip factor large enough to partially compensate for spatial autocorrelation, many stands of cover type were excluded from For topographic influence upon NDVI to be detected examination. in this investigation, a stand must have been large enough to have been sampled at a large distance using appropriate sampling schemes.

The relationship between vegetation and NDVI may only be interpreted as far as the ANOVA tests allow. The relationship between vegetation class and NDVI was strong, and stronger than the relationship between NDVI and incidence angle. The analysis of the relationship between NDVI and vegetation type within incidence classes was not conducted due to a small sample size in some of the class combinations (Table 3.7).

5.2 Concluding remarks

The examination of topographic influence upon NDVI has revealed that incidence angle may cause some "noise" within the signal from vegetation in alpine environments. However, results of this study are limited to one grouping of related vegetation types. The spatial autocorrelation present within the variables inhibits the examination of all vegetation groups. In applications of NDVI for vegetation mapping, topographic influence may be a minimal source of error for large extents of vegetation. Smaller extents of vegetation were excluded from this investigation of the influence of incidence angle on their NDVI.

The results of this study are also limited by the nature of the data set. While validity of the NDVI signal may be assumed for the more dense vegetation classes (i.e., density >60%), caution is warranted for lower density classes. In vegetation classes of lower density, understory vegetation was not included in the analysis. This limitation of the data may explain the large degree of NDVI variability within each of the vegetation classes of low density and the apparent discrepencies for relative NDVI values across classes. Therefore, the most trustworthy result of this investigation is that of vegetation class #15, Lodgepole pine, Limber pine, Spruce Fir, 80-100%, which covers an area of 6380 hectares. Thus, incidence angle introduces noise within the NDVI signal for some expansive vegetation classes of high density $(r^2 = 0.06)$ within a mountainous Tests of the relationship between NDVI and vegetation type indicated a strong, general trend, but were not tested for strength and directionality.

Information about error of any amount within NDVI is valuable for proper interpretation of the index. Investigations into the influence of noise upon the vegetation radiance measured by passive remote sensing satellites have led to the development of soil and atmospheric corrections to radiance values. Modifications to NDVI have addressed the same noise influences caused by the atmosphere and presence of soil adjacent to vegetation. Noise associated with topography has been assumed to be eliminated by the ratio construction of the NDVI. However, variations in the NDVI that are not related to ground cover may lead to misinterpretations of the index in sensitive ecotones.

Scientists are looking to the forest-tundra ecotone as indicators of global change (Baker et al., 1995). The vegetative measures are gathered to monitor changes and adaptations that may indicate large, global changes in climate. The hypothesis is that should climate conditions change, it will affect the forest-tundra ecotones first. Any noise within the vegetation indices must be investigated for the proper interpretation. Within large, homogeneously vegetated terrain, an NDVI variation as large as 6% may be attributed to the topographic effect. Smaller, nonhomogeneous areas were not able to be accurately assessed. Additional investigations are needed to further characterize the remaining topographic effect in mountainous terrain. While a 6% variation for large, homogeneously vegetated areas may appear minimal, it is uncertain from this investigation the extent of the remaining variation for other vegetated mountainous areas, including the forest-tundra ecotone.

5.3 Future research

Additional, more encompassing investigations are needed to solidify these initial findings. The common practice of accepting the topographic compensation characteristics of NDVI needs further questioning for applications in alpine and sub-alpine terrain. future research may include one or several of the following areas: larger site investigation, examination over different areas, different combinations of incidence angles and vegetation/density, and additional directional statistical tests. Such research needs to overcome some of the limitations present within this work. One area of immediate concern is an investigation into the difference between radiance and DN generated NDVI. Radiance values have typically been utilized generate the NDVI from AVHRR data, and are the true basis for correct NDVI calculation. Why are DN values used for some Landsat TM applications of NDVI? The examination of the differences is in order to determine if the practice is justifiable and under what conditions. One additional area of immediate interest is the examination of a suitable extent of each of the vegetation classes, used within this study, for possible topographic influence within NDVI. With such an investigation completed, future users of NDVI may have a better understanding of the topographic noise contained within the index data.





APPENDIX A

Characteristics of Landsat TM (Lillesand and Kiefer, 1994)

			•	
Band		<u>(λ)</u>	Spectrum	Principal Applications
1.	0.45	- 0.52	Blue	Designed for water body
				penetration, making it useful for
				soil/vegetation discrimination,
				forest type mapping, and cultural
				features identification.
2.	0.52	- 0.60	Green	Designed to measure green
				reflectance peak of vegetation for
				vegetation discrimination and
				vigor assessment. Also useful for
				feature identification.
3.	0.63	- 0.69	Red	Designed to sense in a
				chlorophyll absorption region
				aiding in plant species
				differentiation. Also useful for
				cultural feature identification.
4.	0.76	- 0.90	Near IR	Useful for determining
				vegetation types, vigor, and
				biomass content, for delineating
				water bodies, and for soil
				moisture discrimination.
5.	1.55	- 1.75	Mid-IR	Indicative of vegetation moisture
				content and soil moisture. Also
				useful for differentiation of snow
				from clouds.
6.	10.4	- 12.5	Thermal-IR	Useful in vegetation stress
				analysis, soil moisture
				discrimination, thermal mapping
				applications.
7.	2.08	- 2.35	Mid-IR	Useful for discrimination of
				mineraland rock types. Also
				sensitive to vegetation moisture
				content.



APPENDIX B

Meta data of the Landsat image

Scene ID =4254617165 WRS =034/032 ACQUISITION DATE =19890705

SATELLITE =L4 INSTRUMENT =TM PRODUCT TYPE =MAP PRODUCT

TYPE OF GEODETIC PROCESSING =PASS THROUGH

RESAMPLING =CC

ORIENTATION = -3.01

PROJECTION = SOM

USGS PROJECTION # = 21 USGS MAP ZONE = 34

USGS PROJECTION PARAMETERS = 0.63783880000000D+07 0.63569120000000D+08

0.0000000000000D+00 0.980120000000D+08 0.760460242171249D+08

0.000000000000D+00

EARTH ELLIPSOID =INTERNAL_1909

SEMI-MAJOR AXIS =6378388.000

SEMI-MINOR AXIS =6356912.000

PIXEL SIZE =28.50 PIXELS PER LINE =3510 LINES PER IMAGE =3510

UL 1061017.4284W 405234.3400N 533919.000 15534837.000

UR 1050029.0005W 404221.0242N 633787.249 15540093.701

LR 1051411.5080W 394920.7874N 628530.547 15639961.950

LL 1062307.5657W 395326.1515N 528662.299 15634705.249

BANDS PRESENT 1234567

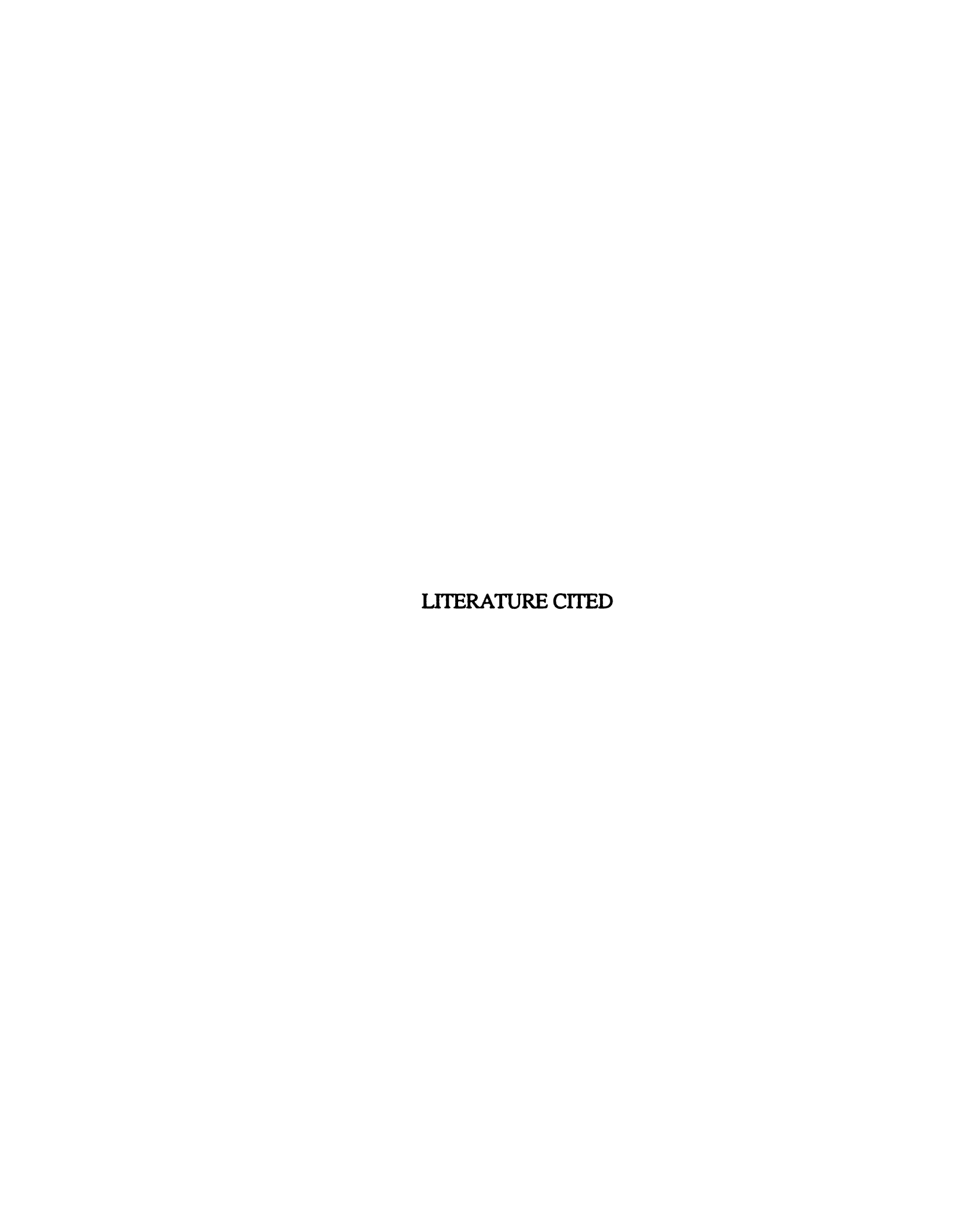
***** FACTOR = 1

RECORD LENGTH =3510

SUN ELEVATION =60

SUN AZIMUTH =118

SCENE CENTER = 570921.416 15590642.306



LITERATURE CITED

- Allen, R. B., R. K. Peet, and W. L. Baker. (1991) Gradient Analysis of latitudinal variation in Southern Rocky Mountain forests. Journal of Biogeography. Vol. 18, 123-139.
- Arno, S. F., and R. P. Hammerly. (1984) Timberline Mountain and Arctic Forest Frontiers. Seattle, Washington: The Mountaineers., 304p.
- Ashburn, P., (1978) The vegetative Index Number and crop identification. Proceedings: The LACIE Symposium. 843-856.
- Baker, W. L., J. J. Honaker, and P. J. Weisberg. (1995) Using Aerial Photography and GIS to Map the Forest-Tundra Ecotone in Rocky Mountain National Park, Colorado, for Global Change Research. Photogrammetric Engineering and Remote Sensing. Vol. 61, No. 3, 313-320.
- Baker, W. L., and P.J. Weisberg. (1995) Landscape Analysis of the Forest-Tundra Ecotone in Rocky Mountain National Park, Colorado. Professional Geographer. Vol. 47, No. 4, 361-375.
- Barbour, M. G., and W. D. Billings. (1988) North American Terrestrial Vegetation. New York: Cambridge University Press., 434p.
- Baret, F. and G. Guyot. (1991) Potentials and Limits of Vegetation Indices for LAI APAR assessment. Remote Sensing of Environment. Vol. 35, 161-173.
- Botkin, D. B., J. E. Estes, R. M. Macdonald, and M. V. Wilson. (1984)

 Studying the Earth's Vegetation from Space. Bioscience.

 Vol. 34, No. 8, 508-514.

- Brown, D. G. (1994) Comparison of Vegetation-Topography Relationships at the Alpine Treeline Ecotone. *Physical Geography*. Vol. 15, No. 2, 125-145.
- Brown, D. G. and T. J. Bara. (1994) Recognition and Reduction of Systematic Error in Elevation and Derivative Surfaces from 7 1/2 Minute DEMS. Photogrammetric Engineering and Remote Sensing. Vol. 60, No. 2, 189-194.
- Brown, J. F., T. R. Loveland, J. W. Merchent, B. C. Reed, and D. O. Ohlen. (1993) Using Multisource Data in Global Land-Cover Characterization: Concepts, Requirements, and Methods. Photogrammetric Engineering and Remote Sensing. Vol. 59, No. 6, 977-987.
- Butera, M. K. (1986) A Correlation and Regression Analysis of Percent Canopy Closure Versus TMS Spectral Response for Selected Forest Sites in San Juan National Forest, Colorado. IEEE Transactions on Geoscience and Remote Sensing. Vol. GE-24, No. 1, 122-129.
- Chiou, C. and R. Hoffer. (1994) A Sequential Sampling
 Approach for Selecting Training Blocks of Landsat TM
 Data in the Rocky Mountain National Park.

 Proceedings: 1995 ACSM/ASPRS Convention and Exposition.
 Vol. 3, 816-825.
- Civco, D. L. (1989) Topographic Normalization of Landsat Thematic Mapper Digital Imagery. Photogrammetric Engineering and Remote Sensing. Vol. 55, No. 9, 1303-1309.
- Colwell, J. E. (1973) Bidirectional spectral reflectance of grass canopies for determination of above ground standing biomass. Ph.D. thesis, University of Michigan, University microfilm. 174 p.
- Crist, E. P., and R. C. Cicone. (1984) A Physically-Based
 Transormation of Thematic Mapper Data-The TM
 Tasseled Cap. IEEE Transactions on Geoscience and Remote
 Sensing. Vol GE-22, NO. 3, 256-263.
- Curran, P. J. (1985) Principles of Remote Sensing. London: Longman Group, 282p.

- Curran, P. J. and N. W. Wardley. (1988) Radiometric leaf area index. International Journal of Remote Sensing. Vol. 9, No. 2, 259-274.
- Deering, D. W., J.W. Rouse, R. H. Haas, and J. A. Schell. (1975)

 Measuring "forage production" of grazing units from

 Landsat MSS data. Proceedings: 10th international

 Symposium Remote Sensing of Environment. Vol. 2, 11691178.
- Dubayah, R., J. Dozier, and F.W. David. (1989) The Distribution of Clear-Sky Radiation Over Varying Terrain. *Proceedings*, *IGARSS* '89, 885-889.
- Dubayah, R., and P. M. Rich. (1995) Topographic solar radiation models for GIS. International Journal of Geographic Information Systems. Vol. 9, No. 4, 405-419.
- EOSAT. (1994) A Process of Radiometry. Eosat News, Vol. 9, No. 2, 10.
- Erdas. (1991) Field Guide. Atlanta: ERDAS, Inc., 250p.
- Frank. T. D. (1988) Mapping Dominant Vegetation
 Communities in the Colorado Rocky Mountain Front
 Range with Landsat Thematic Mapper and Digital
 Terrain Data. Photogrammetric Engineering and Remote
 Sensing., Vol. 54, No. 12, 1727-1734.
- Gausman, H. W. (1977) Reflectance of leaf components. Remote Sensing of Environment., Vol. 6,1-9.
- Goward, S. N., B. Markham, D. G. Dye, W. Dulaney, and J. Yang. (1991)

 Normalized Difference Vegetation Index

 Measurements from the Advanced Very High

 Resolution Radiometer. Remote Sensing of Environment.

 Vol. 35, 257-277.
- Goward, S. N., D. G. Dye, S. Turner, and J. Yang. (1993) Objective assessment of the NOAA global vegetation index data product. International Journal of Remote Sensing. Vol. 14, No. 18, 3365-3394.

- Guttman, G. G. (1991) Vegetation Indices from AVHRR: An Update and Future Prospects. Remote Sensing of Environment. Vol. 35, 121-136.
- Hansen-Bristow, K. J., and J. D. Ives. (1984) Changes in the forest-Alpine Tundra Ecotone: Colorado Front Range. *Physical Geography*. Vol. 5., No. 2, 186-197.
- Holben, B. N., and C. O. Justice. (1980) The Topographic Effect on Spectral Response From Nadir-Pointing Sensors.

 Photogrammetric Engineering and Remote Sensing. Vol. 46, No. 9, 1191-1200.
- Holben, B. N., and C. O. Justice. (1981) An examination of spectral band ratioing to reduce the topographic effect on remotely sensed data. International Journal of Remote Sensing. Vol. 2, No. 2, 115-133.
- Huete, A. R. (1994) An Error and Sensitivity Analysis of the Atmospheric- and Soil-Correcting Variants of the NDVI for the MODIS-EOS. *IEEE Transactions on Geoscience and Remote Sensing.* Vol. 32, No. 4, 897-904.
- Jordon, C. F. (1969) Derivation of leaf area index from quality of light on forest floor. Ecology. Vol. 50, 663-666.
- Kalensky, Z., and D. A. Wilson. (1975) Spectral Signatures of Forest Trees. Proceedings, Third Canadian Symposium on Remote Sensing. 155-171.
- Karaska, M. A., S. J. Walsh, and D. R. Butler. (1986) Impact of environmental variables on spectral signatures acquired by the LANDSAT thematic mapper.

 International Journal of Remote Sensing, Vol. 7, No. 12, 1653-1667.
- Kauth, R. J., and G. S. Thomas. (1976) The Tassel Cap A graphic description of the spectral-temporal development of agricultural crops as seen by Landsat. Proceedings: Symposium on Machine Processing of Remotely Sensed Data. IEEE catalog No. 76, Ch. 1103-1. MPRSD, LARS, Purdue University, West Lafayette, Indiana.

- Kawata, Y., S. Ueno. (1988) Radiometric correction for atmospheric and topographic effects on Landsat MSS images. International Journal of Remote Sensing. Vol. 9, No. 4, 729-748.
- Leprieur, C. E., J. M. Durand, and J. L. Peyron. (1988) Influence of Topography on Forest Reflectance Using Landsat Thematic Mapper and Digital Terrain Data.

 Photogrammetric Engineering and Remote Sensing. Vol. 54, No. 4, 491-496.
- Lillesand, T. M. and R. W. Kiefer. (1994) Remote Sensing and Image Interpretation. New York: John Wiley & Sons, Inc., 750p.
- Meyer, P., K. I. Itten, T. Kellinger, S. Sandmeier, and R. Sandmeier. (1993) Radiometric corrections of topographically induced effects on Landsat TM data in an alpine environment. ISPRS Journal of Photogrammetry and Remote Sensing. Vol. 48, No. 4, 17-28.
- Nelson, R. A. (1953) Plants of Rocky Mountain National Park. Washington, D.C.: U.S. Government Printing Office, 201p.
- Overpeck, J.T., D. Rind, and R. Goldberg. (1990) Climate-induced changes in forest disturbance and vegetation. Nature. Vol. 343, No. 4, 51-53.
- Peet, R. K. (1978a) Forest Vegetation of the Colorado Front Range: Patterns of Species Diversity. Vegetatio. Vol. 37, No. 2., 65-78.
- Peet, R. K. (1978b) Latitudinal variation in southern Rocky Mountain forests. Journal of Biogeography. Vol. 5, 275-289.
- Peet, R. K. (1981) Forest vegetation of the Colorado Front Range. Vegetatio. Vol. 45, No. 1, 3-75.
- Perry, C. R. Jr., and L. F. Lautenschlager. (1984) Functional Equivalence of Spectral Vegetation Indices. Remote Sensing of Environment. Vol. 14, 169-182.

- Price, J. C. (1987) Calibration of Satellite Radiometers and the Comparison of Vegetation Indices. Remote Sensing of Environment. Vol. 21, 15-27.
- Price, J. C. (1993) Estimating Leaf Area Index from Satellite Data. IEEE Transactions on Geoscience and Remote Sensing. Vol. 31, No. 3, 727-734.
- Price, L. W. (1981) Mountains and Man. Berkeley: University of California Press., 506p.
- Proy, C., D. Tanre, and P.Y. Deschamps. (1989) Evaluation of Topographic Effects in Remotely Sensed Data. Remote Sensing of the Environment. Vol. 30, 21-32.
- Richardson, A. J., and C. L. Weigand. (1977) Distinguishing vegetation from soil background information.

 Photogrammetric Engineering and Remote Sensing. Vol. 43, 1541-1552.
- Richmond, G. M. (1960) Glaciation of the east slope of Rocky Mountain National Park, Colorado. Bulletin of the Geological Society of America. Vol. 71, 1371-1382.
- Rouse, J. W., R. H. Haas, J. A. Schell, and D. W. Deering. (1973)

 Monitoring vegetation systems in the great plains
 with ERTS. Third ERTS Symposium, NASA SP-351. Vol. 1,
 309-317.
- Rouse, J. W., R. H. Haas, J. A. Schell, D. W. Deering, and J. C. Harlan. (1974) Monitoring vernal advancement and retrogradation (greenwave effect) of natural vegetation. NASA/GSFC Type III Final Report. Greenbelt, Maryland: Goddard Space Flight Center, 371 p.
- Sellers, P. J. (1985) Canopy reflectance, photosynthesis and transpiration. International Journal of Remote Sensing. Vol. 6, No. 8, 1335-1372.
- Singh, S. M. (1988) Simulation of solar zenith angle effect on global vegetation index (GVI). International Journal of Remote Sensing. Vol. 9, No. 2, 237-248.

- Tarpley, J. D., S. R. Schneider, and R. L. Money. (1984) Global Vegetation Indices from the NOAA-7 Meteorological Satellite. Journal of Climate and Applied Meteorology. Vol. 23, 491-494.
- Teillet, P. M. (1982) On the Slope-Aspect Correction of Multispectral Scanner Data. Canadian Journal of Remote Sensing. Vol. 8, No. 2, 84-106.
- Teillet, P. M. (1986) Image correction for radiometric effects in remote sensing. International Journal of Remote Sensing. Vol. 7, No. 12, 1637-1651.
- Thomas, R. (n.d.) UTM Registration of Landsat TM Data of Rocky Mountain National Park. Colorado State University. unpublished paper. Estes Park, CO. 5p.
- Tucker, C. J. (1979) Red and Photographic Infrared Linear Combinations for Monitoring Vegetation. Remote Sensing of Environment. Vol. 8, 127-150.
- U.S. Geological Survey. (1987) Digital Elevation Models. Data
 User's Guide 5. Reston, Virginia: U.S. Geological Survey, 180p.
- Veblen, T. T., and D. C. Lorenz. (1991) The Colorado Front Range. Salt Lake City, Utah: University of Utah Press. 115p.
- Wardley, N. (1984) Vegetation index variability as a function of viewing geometry. International Journal of Remote Sensing. Vol. 5, No. 5, 861-870.
- Weisberg, P. J., and W. L. Baker. (1995) Spatial variation in Tree Seedling and Krummholz Growth in Forest-Tundra Ecotone of Rocky Mountain National Park, Colorado, USA Arctic and Alpine Research. Vol. 27, No. 2, 116-129.
- Woodham, R. J. and T. K. Lee. (1985) Photogrammetric method for radiometric correction of multispectral scanner data. Canadian Journal of Remote Sensing. Vol. 11, No. 2, 132-161.

